

Experimental realization of optomechanically induced non-reciprocity

Z. Shen,^{1,2} Y.-L. Zhang,^{1,2} Y. Chen,^{1,2} C.-L. Zou,^{1,2,3,*} Y.-F. Xiao,⁴
X.-B. Zou,^{1,2} F.-W. Sun,^{1,2} G.-C. Guo,^{1,2} and C.-H. Dong^{1,2,†}

¹Key Laboratory of Quantum Information, Chinese Academy of Sciences,
University of Science and Technology of China, Hefei 230026, P. R. China.

²Synergetic Innovation Center of Quantum Information and Quantum Physics,
University of Science and Technology of China, Hefei, Anhui 230026, P. R. China.

³Department of Electrical Engineering, Yale University, New Haven, Connecticut 06511, USA

⁴State Key Laboratory for Mesoscopic Physics and School of Physics,
Peking University, Beijing 100871, People's Republic of China.

Non-reciprocal devices, such as circulators and isolators, are indispensable components in classical and quantum information processing in an integrated photonic circuit [1]. Aside from those applications, the non-reciprocal phase shift is of fundamental interest for exploring exotic topological photonics [2], such as the realization of chiral edge states and topological protection [3, 4]. However, incorporating low optical-loss magnetic materials into a photonic chip is technically challenging [5]. In this study, we experimentally demonstrate non-magnetic non-reciprocity using optomechanical interactions in a whispering-gallery microresonator, as proposed by Hafezi and Rabl [6]. Optomechanically induced non-reciprocal transparency and amplification are observed, and a non-reciprocal phase shift of up to 40 degrees is demonstrated in this study. The results of this study represent an important step towards integrated all-optical controllable isolators and circulators, as well as non-reciprocal phase shifters.

In recent years, there has been growing interest in the realization of non-reciprocal photonic devices without magnetic material. To create genuine non-reciprocal devices, it is necessary to break the Lorentz reciprocity [7]. The methods that attempt to achieve this goal primarily rely on two mechanisms: the effect due to a moving medium or reference frame, and the nonlinear optical effect. The Sagnac effect utilizes the first mechanism and can induce non-reciprocal phase shift for a photon propagating in a rotating non-inertial frame of reference [8]. In particular, Fleury et al. [9] reported the sound analogue of isolation due to a circulating fluid medium. However, the optical Sagnac effect requires a long optical path, which is not suitable for a photonic chip.

Based on the nonlinear optical effect, the non-reciprocity of a photon can be achieved by interacting with traveling wave excitations or equivalent spatiotemporal modulation [10–12]. For example, a directional

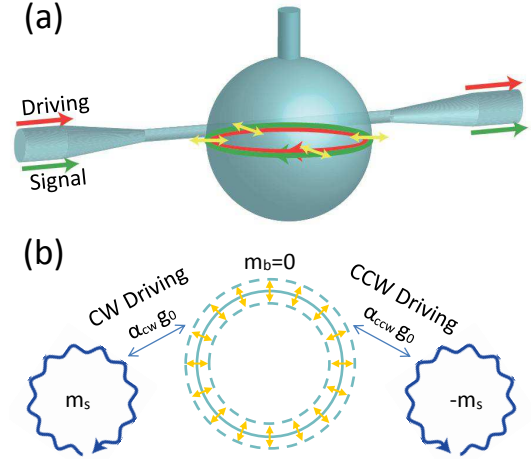


FIG. 1: Schematic illustration of optomechanically induced non-reciprocity. (a) A strong driving field enhances the optomechanical coupling between a vibrational mode and the co-propagating optical mode inside a microcavity. (b) The schematic of clockwise and counter-clockwise optical mode coupling with the breathing mode.

traveling acoustic wave can only efficiently couple with light that propagates forward or backward due to Brillouin scattering, which leads to time-reversal symmetry breaking of light [13–15]. A similar effect can also be realized with a directional photon-photon interaction in a nonlinear micro-ring resonator [16]. However, the energy conservation and momentum matching conditions must be satisfied for all involved modes, resulting in challenges for dispersion engineering and fabrication of photonic structures. There are also efforts to create an optical isolator via Kerr-like nonlinearity induced bistability, but the performance for a single-photon-level signal and the isolation from weak backward noise are under debate [17].

In this article, we report the experimental demonstration of optomechanically induced non-reciprocity in a silica microsphere resonator. This approach was first suggested by Hafezi and Rabl [6] and states that an optical mode dispersively couples with a symmetric radial breathing mechanical mode. A signal photon can only be affected when it propagates in the same direction as the driving laser. Compared to the triple resonant inter-

*Electronic address: clzou321@ustc.edu.cn

†Electronic address: chunhua@ustc.edu.cn

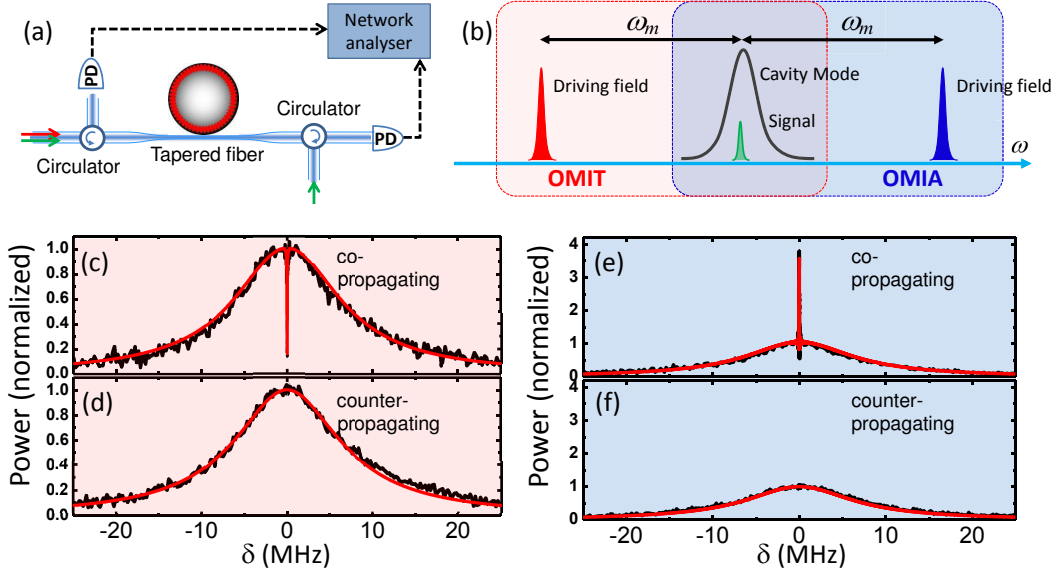


FIG. 2: **Optomechanically induced transparency (OMIT) and amplification (OMIA)**. (a) A simplified schematic of the experimental setup with a co- or counter-propagating signal in a silica microsphere. (b) Spectral position of the driving and signal field in OMIT and OMIA processes. (c-d) The emission power spectra in the OMIT response are obtained using a co- and counter-propagating signal pulse. The incident driving power is 10 mW. The solid red lines are the results of calculations using the parameters $\omega_m/2\pi = 88.54$ MHz, $\kappa/2\pi = 15$ MHz, $\gamma_m/2\pi = 22$ kHz, and $C_{cw} = 1.5$, respectively. (e-f) The emission power spectra in the OMIA response are obtained using a co- and counter-propagating signal pulse. The incident driving power is 5.5 mW. The solid red lines are the results of calculations using the parameters $\omega_m/2\pi = 88.54$ MHz, $\kappa/2\pi = 15$ MHz, $\gamma_m/2\pi = 22$ kHz, and $C_{cw} = -0.8$, respectively.

action, which consists of two optical modes and one traveling acoustic wave, in Brillouin scattering [13–15], non-reciprocity can be achieved for any whispering gallery modes in the cavity considered in this study, which is more favorable for future applications. Note that this optomechanically induced non-reciprocity is applicable to all traveling wave resonators and can be easily implemented on photonic chips. With the mechanical vibrations being cooled to their ground states, applications in the quantum regime, such as single-photon isolators and circulators, also become possible.

Figure 1(a) schematically illustrates a traveling wave optomechanical system that consists of a whispering gallery microresonator that is evanescently coupled with a tapered fiber [18–20]. The traveling wave nature of the microresonator produces a rise in the degenerate clockwise (CW) and counter-clockwise (CCW) traveling-wave whispering-gallery modes (WGMs), which can also be represented by the orbital angular momentums m and $-m$, respectively. Similarly, the mechanical modes in such axial symmetric geometry have an orbital angular momentum m_b , where $m_b = 0$ represents the breath vibration mode, where the equator of the sphere expands and compresses uniformly. The variation of the cavity radius leads to the modification of the resonant frequency of all optical modes [18, 19, 21], which can be described by the dispersive optomechanical interaction Hamiltonian [6]:

$$H_{int} = g_0(a_{cw}^\dagger a_{cw} + a_{ccw}^\dagger a_{ccw})(b + b^\dagger), \quad (1)$$

where $a_{cw(ccw)}$ and b denote the Bosonic operators of the CW(CCW) optical mode and mechanical mode, respectively. For such an interaction, only a single optical mode (either a_{cw} or a_{ccw}) is involved; therefore, the properties of the driving and signal optical fields should be identical, except for the frequency difference. Thus, the CW(CCW) driving field can only stimulate the interaction between a phonon and a CW(CCW) signal photon, as shown in Fig. 1(b). This relation between the driving-signal directions can also be interpreted using the conservation of orbit angular momentum $m_s - m_d = m_b = 0$, where m_s and m_d denote the momentum for the signal photon and driving laser, respectively. As a result, the directional driving field breaks the time-reversal symmetry and leads to non-reciprocal transmittance for the signal light: the co-propagating signal photons can be coherently coupled with phonons, while the coupling between counter-propagating photons and the phonon is negligible.

The experimental demonstration of the optomechanically induced non-reciprocity is performed using the experimental setup shown in Fig. 2(a). The driving laser excites the CW optical mode, while either CW or CCW signal photons are sent to the cavity (see the Supplementary information for more details with regard to the experimental setup). In a sphere with a diameter of approximately $36 \mu\text{m}$, we choose a high quality factor WGM near 780 nm (linewidth $\kappa/2\pi = 15$ MHz). The radial breathing mechanical mode in this sphere has a frequency of

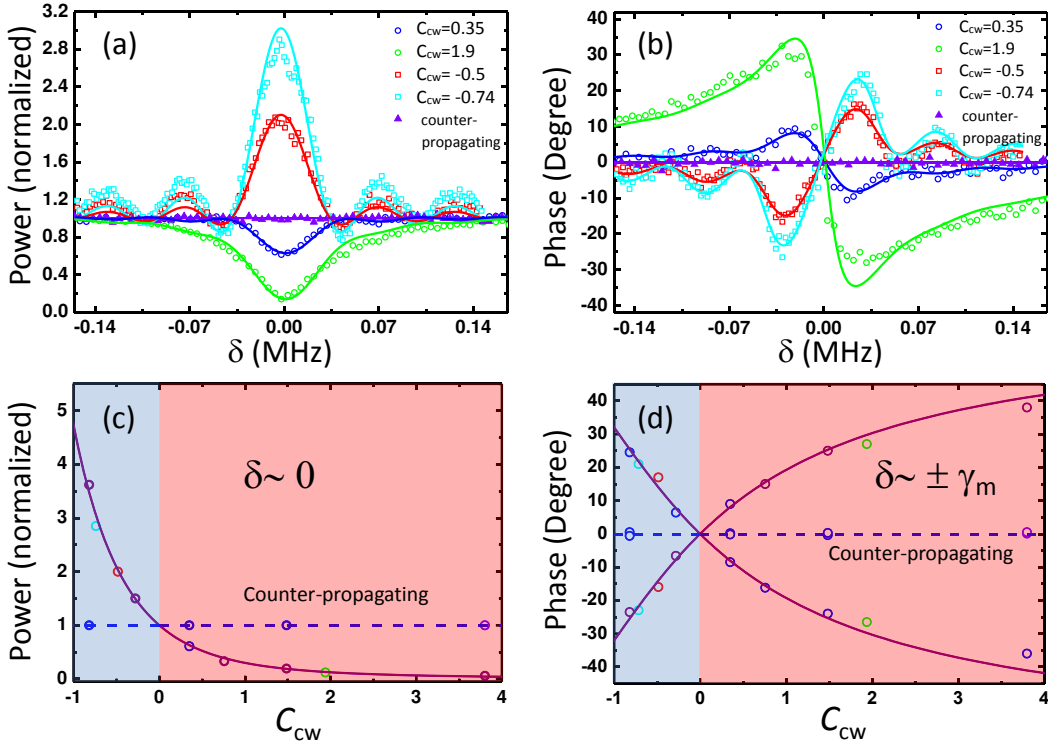


FIG. 3: **Optomechanically induced non-reciprocal transmission and phase shift.** (a) The typical emission power from the microcavity with the co-propagating (i.e., circle for OMIT and square for OMI) and counter-propagating signal (i.e., triangle) and the corresponding phase response (b) at different driving powers. The solid lines are the results of calculations using $C_{cw} = -0.74, -0.5, 0, 0.35, 1.9$. (c) The spectral depth of the transparency window or spectral peak of the opacity peak as a function of the cooperativity C_{cw} . (d) The shift phase obtained at the detuning $\delta = \pm \gamma_m$. The lines in (c-d) represent the theoretically expected values.

$\omega_m/2\pi = 88.5$ MHz and a linewidth of $\gamma_m/2\pi = 22$ kHz.

Figure 2(b) shows the two configurations of the driving field. For the driving field that is red-detuned from the cavity mode by ω_m , an effective photon-phonon beam-splitter-like interaction ($a_{cw}^\dagger b + a_{cw} b^\dagger$) would lead to coherent conversion and induce a transparent window in the cavity field spectrum [22, 23]. In this study, we send a short drive laser and signal pulse (duration $\tau_p = 18 \mu\text{s}$) to measure the transient optomechanical coupling to avoid thermal instability in the microsphere. The experimental result in Fig. 2(c) shows a sharp transparency window for co-propagating signal photons, demonstrating the destructive interference between the signal field and the optical field generated from the anti-Stokes scattering process. Conversely, the spectrum of the counter-propagating signal in Fig. 2(d) does not show such an effect, which is indicative of optomechanically induced non-reciprocity. The spectra still agree with the theoretical predictions of the steady-state intracavity field [19]:

$$a_{cw}(\delta) = \frac{-\sqrt{\kappa_{in}} \epsilon_{s,cw}}{i\delta - \frac{\kappa}{2} \left(1 + \frac{C_{cw}}{1 - i2\delta/\gamma_m}\right)}, \quad (2)$$

$$a_{ccw}(\delta) = \frac{-\sqrt{\kappa_{in}} \epsilon_{s,ccw}}{i\delta - \frac{\kappa}{2}}. \quad (3)$$

where $C_{cw} = \frac{4|G_{cw}|^2}{\kappa\gamma_m}$ is the cooperativity; $G_{cw} = \sqrt{N_d}g_0$ is the effective optomechanical coupling rate; N_d is the CW driving intracavity photon number; $\epsilon_{s,cw}$ and $\epsilon_{s,ccw}$ are the weak signal amplitudes of the CW- and CCW-circulating optical modes, respectively; δ is the detuning between the signal and cavity field; and κ_{in} is the coupling rate between the microfiber and microsphere. For a critically coupled optical mode, the observed intracavity fields for the CW and CCW signal corresponding to non-reciprocal transmissions of the CW and CCW signal are 0 and 1 around $\delta \sim 0$, respectively.

For the driving field that is blue-detuned from the cavity mode by ω_m (i.e., driving frequency $\omega_d = \omega_c + \omega_m$), an effective photon-phonon pair generation process ($a_{cw}^\dagger b^\dagger + a_{cw} b$) would lead to optomechanically induced amplification. Figures 2(e) and (f) present the corresponding experimental results, which show non-reciprocal amplification of the signal. The sequences of driving laser and signal pulses are the same as before. Here, the experimental results are fitted by the modified transient intracavity field spectra because of the unsteady state optomechanical coupling even with $18 \mu\text{s}$ driving pulse at

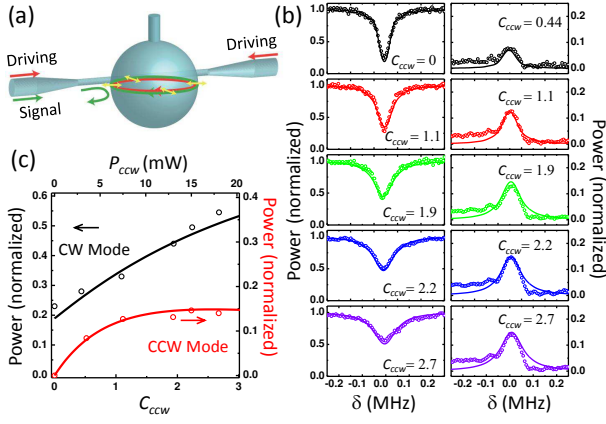


FIG. 4: **Optical mode conversion between two oppositely propagating optical fields.** (a) Two driving fields are applied simultaneously to induce the reflection of the signal. (b) The cavity emission power spectra in the CW direction and the reflected power spectra in the CCW direction vary with the cooperativity C_{ccw} . The peak power of the CW driving pulse is 10 mW, corresponding to $C_{cw} = 1.5$. (c) Emission powers from the CW mode (black circles) and CCW mode (red circles) at $\delta = 0$ as a function of C_{ccw} . The solid lines in (b-c) are results of the theoretical calculations.

blue sideband:

$$a_{cw}(\delta) = \frac{-\sqrt{\kappa_{in}}\epsilon_{s,cw}}{i\delta - \frac{\kappa}{2}\left(1 + \frac{C_{cw}}{1 - i2\delta/\gamma_m}\right)} [1 + F(\tau_p)], \quad (4)$$

with the transient modification $F(t) = \frac{2C_{cw}Exp(i\delta t - (\kappa + \gamma_m)t/4)}{1 - i2\delta/\gamma_m} \sinh\left[\frac{t\sqrt{(\kappa + \gamma_m)^2/4 - \kappa\gamma_m(1 + C_{cw})}}{2}\right]$.

In this study, $C_{cw} = -\frac{4|G_{cw}|^2}{\kappa\gamma_m}$ has a negative sign, which would effectively narrow the linewidth of the cavity and amplify the intracavity signal.

To obtain a more quantitative analysis of the optomechanically induced non-reciprocity, the detailed spectra for different experimental conditions are shown in Fig. 3(a). For blue detuning, the peak height increases and the linewidth decreases with the driving power. For red detuning, the transparent depth and linewidth both increase with the driving power. The intensity at $\delta = 0$ and the corresponding cooperativity C_{cw} are summarized and plotted in Fig. 3(c). The intensity of the co-propagating signal agrees with the prediction, while the counter-propagating signal is found to be independent of C_{cw} .

The non-reciprocal transmittance of the signal can also be inferred from the phase because $\arg(a_{cw}(\delta))$ in Eq. (2) varies with the detuning and C_{cw} . The measured phase is plotted in Fig. 3(b); the difference between the co-propagating and counter-propagating signal unambiguously shows the non-reciprocal phase shifter due to the optomechanical interaction. The extracted phases at $\delta = \pm\gamma_m$ that are plotted in Fig. 3(d) agree with the theory. The maximum phase shift achieved in the proposed experiment is approximately 40 degrees. The oscillations

around the opacity peak in Fig. 3(a) and the corresponding phase response in Fig. 3(b) are observed due to the transient response of the optomechanical system [24], as described by $F(t)$.

Optomechanically induced non-reciprocity is actually controllable using two oppositely propagating driving fields that excite the CW and CCW modes simultaneously. As a result of the interesting interplay between the three coupled modes (Fig. 1(b)), there is an optomechanically dark mode [19] (i.e., a superposition of the CW and CCW modes), which enables the conversion of optical fields from the CW mode to the CCW mode. To test the optical mode conversion, we fixed the CW driving power at 10 mW and varied the CCW driving power from 0 to 18 mW, while the input signal coupled only to the CW mode. As shown in Fig. 4(b), the excitation of the CW mode increases with increasing C_{ccw} , and the OMIT dip for this mode vanishes and is accompanied by a spectral broadening of the dip. There is light reflected from the system with a bandwidth smaller than 100 kHz; its peak power at $\delta \sim 0$ also increases with C_{ccw} . The theoretical model predicts that $a_{cw} \propto \frac{1+C_{ccw}}{1+C_{cw}+C_{ccw}}$ and $a_{ccw} \propto \frac{\sqrt{C_{cw}C_{ccw}}}{1+C_{cw}+C_{ccw}}$ for the CW signal, which agrees with the experiment results shown in Fig. 4(c). Compared to the CCW signal, for which $a_{ccw} \propto \frac{1+C_{cw}}{1+C_{cw}+C_{ccw}}$ and $a_{cw} \propto \frac{\sqrt{C_{cw}C_{ccw}}}{1+C_{cw}+C_{ccw}}$, the co-propagating intracavity excitation and transmission are non-reciprocal if $C_{cw} \neq C_{ccw}$, while the signal reflection is always reciprocal. Therefore, the system behaves as a controllable narrowband reflector with non-reciprocal transmittance, which might be interesting for future studies.

To summarize, optomechanically induced non-reciprocity is experimentally demonstrated for the first time in this study. The underlying mechanism of the non-reciprocity demonstrated in this study is actually universal and can be generalized to any traveling wave resonators via dispersive coupling with a mechanical resonator, such as the integrated ring-type microresonator coupled with a nanobeam [25]. Considering that higher cooperativity and cascading of the non-reciprocal devices are possible in a photonic integrated chip, optomechanically induced non-reciprocity has applications in integrated photonic isolators and circulators [26], which will play important roles in a hybrid quantum Internet [27].

Note added: When finalizing the manuscript, we became aware of the related work of F. Ruesink et al. [28], who demonstrated optomechanically induced non-reciprocal transmission in a microtoroid resonator.

Acknowledgments

The authors would like to thank H. Wang and X. Guo for discussions. The work was supported by the Strategic Priority Research Program (B) of the Chinese Academy of Sciences (Grant No. XDB01030200), the

National Natural Science Foundation of China (Grant No.61308079, 61575184 and 11474011), Anhui Provincial Natural Science Foundation (Grant No. 1508085QA08), the Fundamental Research Funds for the Central Univer-

sities.

-
- [1] Shoji, Y. Mizumoto, T. Magneto-optical nonreciprocal devices in silicon photonics. *Sci. Technol. Adv. Mater.* 15, 014602 (2014).
- [2] Lu, L., Joannopoulos, J. D. Soljacic, M. Topological photonics. *Nat. Photonics* 8, 821–829 (2014).
- [3] Wang, Z., Chong, Y., Joannopoulos, J. D. Soljacic, M. Observation of unidirectional backscattering-immune topological electromagnetic states. *Nature* 461, 772–775 (2009).
- [4] Hafezi, M., Demler, E. a., Lukin, M. D. Taylor, J. M. Robust optical delay lines with topological protection. *Nat. Phys.* 7, 907–912 (2011).
- [5] Bi, L. et al. On-chip optical isolation in monolithically integrated non-reciprocal optical resonators. *Nat. Photonics* 5, 758–762 (2011).
- [6] Hafezi, M. Rabl, P. Optomechanically induced nonreciprocity in microring resonators. *Opt. Express* 20, 7672 (2012).
- [7] Jalas, D. et al. What is - and what is not - an optical isolator. *Nat. Photonics* 7, 579-582 (2013).
- [8] Post, E. J. Sagnac effect. *Rev. Mod. Phys.* 39, 475–493 (1967).
- [9] Fleury, R., Sounas, D. L., Sieck, C. F., Haberman, M. R. Alu, A. Sound Isolation and Giant Linear Nonreciprocity in a Compact Acoustic Circulator. *Science* 343, 516-519 (2014).
- [10] Yu, Z. Fan, S. Complete optical isolation created by indirect interband photonic transitions. *Nat. Photonics* 3, 91-94 (2009).
- [11] Lira, H., Yu, Z., Fan, S. Lipson, M. Electrically Driven Nonreciprocity Induced by Interband Photonic Transition on a Silicon Chip. *Phys. Rev. Lett.* 109, 033901 (2012).
- [12] Tzuang, L. D., Fang, K., Nussenzveig, P., Fan, S. Lipson, M. Non-reciprocal phase shift induced by an effective magnetic flux for light. *Nat. Photonics* 8, 701(2014).
- [13] Kang, M. S., Butsch, A. Russell, P. S. J. Reconfigurable light-driven opto-acoustic isolators in photonic crystal fibre. *Nat. Photonics* 5, 549-553 (2011).
- [14] Dong, C.-h. et al. Brillouin-scattering-induced transparency and non-reciprocal light storage. *Nat. Commun.* 6, 6193 (2015).
- [15] Kim, J., Kuzyk, M. C., Han, K., Wang, H. Bahl, G. Non-reciprocal Brillouin scattering induced transparency. *Nat. Phys.* 11, 275-280 (2015).
- [16] Guo, X., Zou, C.-L., Jung, H. Tang, H. X. Nonreciprocal nonlinear optic induced transparency and frequency conversion on a chip. arXiv 1511.08112 (2015).
- [17] Shi, Y., Yu, Z. Fan, S. Limitations of nonlinear optical isolators due to dynamic reciprocity. *Nat. Photonics* 9, 388-392 (2015).
- [18] Park, Y.-S. Wang, H. Resolved-sideband and cryogenic cooling of an optomechanical resonator. *Nat. Phys.* 5, 489-493 (2009).
- [19] Dong, C., Fiore, V., Kuzyk, M. C. Wang, H. Optomechanical dark mode. *Science* 338, 1609-13 (2012).
- [20] Schliesser, A. Kippenberg, T. J. Cavity Optomechanics with Whispering-Gallery-Mode Microresonators. In *Cavity Optomech.*, volume 24, 121-148. Springer Berlin Heidelberg, Berlin, Heidelberg (2014).
- [21] Ma, R. et al. Radiation-pressure-driven vibrational modes in ultrahigh-Q silica microspheres. *Opt. Lett.* 32, 2200 (2007).
- [22] Weis, S. et al. Optomechanically induced transparency. *Science* 330, 1520 (2010).
- [23] Safavi-Naeini, a. H. et al. Electromagnetically induced transparency and slow light with optomechanics. *Nature* 472, 69 (2011).
- [24] Dong, C., Zhang, J., Fiore, V. Wang, H. Optomechanically induced transparency and self-induced oscillations with Bogoliubov mechanical modes. *Optica* 1, 425 (2014).
- [25] Li, M., Pernice, W. H. P. Tang, H. X. Reactive Cavity Optical Force on Microdisk-Coupled Nanomechanical Beam Waveguides. *Phys. Rev. Lett.* 103, 223901 (2009).
- [26] Fu, W. et al. Integrated optical circulator by stimulated Brillouin scattering induced non-reciprocal phase shift. *Opt. Express* 23, 025118 (2015).
- [27] Dong, C., Wang, Y. Wang, H. Optomechanical interfaces for hybrid quantum networks. *National Science Review* 2, 510-519 (2015).
- [28] Ruesink, F. Verhagen, E. Optomechanically induced non-reciprocity. In *Mechanical systems in the quantum regime* (Gordon Research Seminar) (2016).